Journal of Bioenergetics and Biomembranes, Vol. 36, No. 4, August 2004 (© 2004)

Using ^{31}P NMR Spectroscopy at 14.1 Tesla to Investigate PARP-1 Associated Energy Failure and Metabolic Rescue in Cerebrocortical Slices

Jianying Zeng,[1] Kiyoshi Hirai,[1] Guo-Yuan Yang,[1] Weihai Ying,[2] Raymond A. Swanson,[2] Mark Kelly,[3] Moriz Mayer,[3] Thomas L. James,[3] and Lawrence Litt[1,4]

Received April 23, 2004; accepted May 7, 2004

PARP-1 activation by H_2O_2 in an acute preparation of superfused, respiring, neonatal cerebrocortical slices was assessed from PAR-polymer formation detected with immunohistochemistry and Western blotting. ^{31}P NMR spectroscopy at 14.1 Tesla of perchloric acid slice extracts was used to assess energy failure in a 1-h H_2O_2 exposure as well as in a subsequent 4-h recovery period where the superfusate had no H_2O_2 and specifically chosen metabolic substrates. Although more data are needed to fully characterize different bioenergetic responses, a high NMR spectral resolution (PCr full-width at half-max $\approx$ .01 ppm) and narrow widths for most metabolites ($<$.2 ppm) permitted accurate quantifications of spectrally resolved resonances for ADP, ATP, NAD^+/NADH, and other high energy phosphates. It appears possible to use brain slices to quantitatively study PARP-related, NAD-associated energy failure, and rescue with TCA metabolites.

KEY WORDS: Brain slice; NMR spectroscopy; poly-(ADP-ribose)-polymerase; ATP; nicotinamide adenine dinucleotide; ^{31}P.

INTRODUCTION

Studies of molecular mechanisms of hypoxic/ischemic brain injury often focus on the important role of an abundant nuclear enzyme, poly-(ADP-ribose)-polymerase-1 (PARP-1, PARP, EC 2.4.2.30). For several years in vivo studies have firmly demonstrated that in cerebral ischemia inactivation of PARP-1 reduces infarct size and improves outcome (see, for example, Eliasson *et al*., 1997; Endres *et al*., 1997). In healthy cells PARP-1, when activated in the nucleus by minor DNA damage, initiates repairs by first cleaving NAD^+ (β-nicotinamide adenine dinucleotide) into its components, nicotinamide and ADP-ribose, and then attaching anywhere from a few to a few hundred ADP-ribose polymers onto histones and various proteins. It also polyribosylates itself, causing its own inactivation. Recent comprehensive reviews of PARP include those by D'Amours *et al*., 1999; Herceg and Wang, 2001; Virag and Szabo, 2002; and Hassa and Hottiger, 2002. In healthy cells having only a small amount of DNA damage, poly-ADP-ribosylation efficiently initiates the DNA repair that occurs after enzymes in the PARG family (poly-ADP-ribose glycohydrolase) remove the poly-ADP-ribose units, undoing PARP's work. Thus poly-ADP-polyribosylation by PARP-1 lasts only for a brief time, serving as a transient activation signal to enzymes of repair.

Although there still is an incomplete understanding of the mechanisms by which PARP-1 exacerbates cell injury during and after oxygen deprivation, it is not unusual to see NAD^+ depletion listed as an important culprit. NAD^+ is a key redox participant in glycolysis and the TCA cycle, and it has been suggested that heavily damaged DNA triggers intense overconsumption of NAD^+ via

[1] Department of Anesthesia, University of California at San Francisco, San Francisco, California.
[2] Department of Neurology, University of California at San Francisco and Veterans Affairs Medical Center, San Francisco, California.
[3] Department of Pharmaceutical Chemistry, University of California at San Francisco, San Francisco, California.
[4] To whom correspondence should be addressed: Lawrence Litt, PhD, MD, Department of Anesthesia, University of California, San Francisco Box 0648, 521 Parnassus Avenue, Room C455, San Francisco, California 94143-0648; e-mail: llitt@itsa.ucsf.edu.

back-to-back action of PARP-1 and PARG, i.e., by futile cycling where PARP repeatedly attaches ADP-ribose units and PARG repeatedly removes them. Additionally, NAD^+ restoration adds to energy depletion, because four ATP molecules are required to regenerate one NAD^+ (Zhang *et al.*, 1994). PARP-induced energy failure with cytosolic NAD^+ depletion—along with metabolic rescue—were recently demonstrated in neuron and astrocyte cell culture studies (Ying *et al.*, 2002), where neuron and astrocyte monolayers were treated with *N*-methyl-*N*-nitro-*N*-nitrosoguanidine (MNNG) or with H_2O_2, agents known to activate PARP. Cell death in those studies was prevented or reversed by administration of PARP inhibitors or TCA cycle substrates such as pyruvate, glutamine, and α-ketoglutarate. It is important to know if this kind of PARP-associated energy failure and rescue are relevant to events occurring in vivo, where NAD^+/NADH reserves might be more robust. Realizing that our acute brain slice preparation provides tissue conditions closer to those in vivo, and that high resolution NMR spectroscopy is an outstanding tool for investigating metabolic phenomena, we sought a brain slice protocol that would exhibit PARP-associated energy failure and rescue, possibly with features recognizably similar to those seen in cell culture studies. This paper reports our findings.

MATERIALS AND METHODS

Perfused Brain Slice Preparation and Bench Top Experiments

Our protocol for obtaining, recovering, and maintaining respiring brain slices was approved by the UCSF Committee on Animal Research. Details can be found in recent publications by our group (Hirai *et al.*, 2002; Litt *et al.*, 2003). Briefly, in each experiment we used 20 cerebrocortical slices (350-μm thick) that were obtained from ten 7-day-old Sprague-Dawley rats after decapitation during isoflurane anesthesia. Slices were maintained in a 15-mL conical tube through which there was superfusion with fresh, oxygenated artificial cerebrospinal fluid (oxy-ACSF) that consisted of a modified Krebs balanced salt solution containing 124 mmol/L NaCl, 5 mmol/L KCl, 1.2 mmol/L KH_2PO_4, 1.2 mmol/L $MgSO_4$, 1.2 mmol/L $CaCl_2$, 26 mmol/L $NaHCO_3$, and 10 mmol/L glucose. The bicarbonate buffer for oxy-ACSF underwent continuous bubbling with a 95% O_2/5% CO_2 gas mixture and maintained constant values of PCO_2 (40 mmHg), PO_2 (600–650 mmHg) and pH (7.4). The superfusion chamber was immersed in a water bath that was kept at 37°C. The oxy-ACSF flow rate was 10–15 mL/min, and slices underwent 3 h of metabolic recovery before experiments began.

Experimental Design for Activating PARP and Adding Treatments

PARP activation was induced via oxidative stress from superfusion with ACSF that contained hydrogen peroxide (H_2O_2, 2 or 4 mM). The H_2O_2 exposure was terminated after 1 h at which time a 4-h metabolic rescue was initiated. Parallel experiments were conducted with the PARP inhibitor 3-aminobenzamide (3AB, 3 or 5 mM, Sigma Chemical Co, St. Louis, MO) being present during H_2O_2 exposure. In these experiments, 3AB superfusion started 1 h prior to H_2O_2 administration and stopped when H_2O_2 exposure terminated. Immediately prior to H_2O_2 exposure the ACSF glucose concentration was lowered to 0 or 2 mM (from 10 mM). During the rescue period the ACSF contained glucose, or pyruvate (Sigma Chemical Co, St. Louis, MO), or a mixture of the two, or no energy substrate. At four time points slices were removed from the perfusion chamber, washed rapidly in 4°C normal saline, immediately frozen in liquid nitrogen, and stored at −80°C for subsequent NMR studies or Western blots: 1) $t = 0$ h, just before the 1-h H_2O_2 exposure; 2) $t = 20$ min, during H_2O_2 exposure; 3) $t = 60$ min, at the end of H_2O_2 exposure; and 4) $t = 5$ h, after 4 h of posttreatment with oxy-ACSF that contained pyruvate.

NMR Measurements—Perchloric Acid (PCA) Extraction of Slice Metabolites

Seven frozen slices from each time point were placed in a mortar containing liquid nitrogen (LN_2) and a pestle at the same temperature (−196°C). The slices were then pulverized under LN_2, and resulting fine powder was placed in a centrifuge tube containing 5 mL of 12% perchrolic acid at 4°C. After washing the tube wall with an additional 2 mL of 4°C perchloric acid, the mixture was homogenized at 4°C with an ultrasonicater (Kimble-Kontes, Vineland, NJ). After 20-min centrifugation of the mixture at 15,000 rpm at 4°C the supernatant was collected, while the pellet was resuspended with 2 mL of distilled water, ultrasonicated, and again centrifuged at 4°C. The second supernatant was added to the first, with the final mixture then being carefully, monotonically neutralized with KOH (8, 1, and 0.1 N) to the pH range of 7.0–7.4 (with no overshoots). An additional centrifugation eliminated perchlorate salts. The final supernatant was then lyophilized (BenchTop 2K Lyophilizer, Virtis, Gardiner, NY) and refrigerated at −80°C until just prior to NMR spectroscopy.

At that time each lyophilized PCA extract was dissolved in 435 μL of 99.9% D_2O. Centrifugation then followed, after which 300 μL of supernatant was taken and given a 1 mg addition of EDTA and a few additional drops of NaOD to make the final pD $\approx$ 7.0–7.2. Two microliters of 330 mM methylene diphosphonate (MDP) and 1 μL of 700 mM 3-(trimethylsilyl)-tetradeuterosodium propionate (TSP) were added as internal NMR reference compounds having final concentrations of 2.2 and 2.33 mM, respectively. The pD was again adjusted to 7.0–7.4, if necessary, and final quantity was then loaded into a 5 mm Shigemi NMR tube (Shigemi Co, Tokyo, Japan).

NMR Measurements—^{31}P Spectroscopy at 14.1 Tesla

NMR studies were performed in the new Mission Bay UCSF Magnetic Resonance Laboratory (http://picasso.nmr.ucsf.edu) using a 14.1-Tesla (600-MHz) Varian INOVA spectrometer and a customized, multinuclear Z-SPECT radiofrequency probe that was optimized for this project (3NG600-8, Nalorac Corporation, Martinez, CA 94553). Basic one-pulse, 90° tip angle, RF sequences were used for obtaining ^{1}H spectra at 599.92 MHz and ^{31}P spectra at 242.86 MHz. The extra homogeneity provided by the Shigemi NMR tubes and the Varian INOVA shimming software typically resulted in spectral linewidths of .004 ppm FWHM for ^{1}H water protons and .01 ppm FWHM for ^{31}P in phosphocreatine. Phosphorous spectra were obtained typically with a 1-s interpulse delay during 8-h runs.

Western Blot Analysis of Poly(ADP-ribose) Polymers as a Monitor of PARP-1

After placing three slices ($\approx 3 \times 50$ mg wet weight) from each time point in an ice-cold lysis buffer (20 mM HEPES-KOH at pH 7.5, 10 mM KCl, 1.5 mM $MgCl_2$, 1 mM EDTA, 1 mM EGTA, 0.1% SDS, 1 $\times$ Protease inhibitor cocktail) the mixture was sonicated and then centrifuged (10,000g) at 4°C for 20 min. The resulting supernatant was used as the whole cell protein extraction. After determining protein concentrations by the Bradford method (Bio-Rad, Hercules, CA), 60 μg of protein from each sample underwent sodium dodecyl sulfate-polyacrylamide electrophoresis (SDS-PAGE) on a 4–12% Bis Tris gel (Invitrogen, Carlsbad, CA). Separated proteins were transferred from the gel to a polyvinylidine difluoride membrane (Millipore, Bedford, MA) which was then incubated for 1 h in a blocking buffer containing 5% blotting grade nonfat dry milk in 0.1 M sodium phosphate buffer (pH 7.4). Next the membrane was incubated overnight with mouse anti-PAR monoclonal antibody 4335-MC (Trevigen, Gaithersburg, MD) diluted 1:1000, washed, and incubated for 1 h with a 1:10,000 dilution of peroxidase conjugated anti-mouse lgG (Amersham Life Science, Piscataway, NJ). Bound antibody was visualized by chemiluminescence. As a check on protein loading, β-actin, a typical "housekeeping protein," was quantified after stripping the membrane and then following the same steps described above. PAR polymer formation was quantified by optical density (OD) measurements of intensities in the molecular weight region between 80 and 210 kDa. The OD of β-actin was measured as the internal control. Then the following ratio of ODs was determined for each time point: (PAR polymer)/(β-actin). Measured intensities for different blots on different days were normalized using quantifications of bands from a reference lane on each blot where the same amount of protein was always loaded from the same source.

RESULTS

In initial attempts to induce brain slice intracellular energy failure and NAD^+ depletion we used MNNG

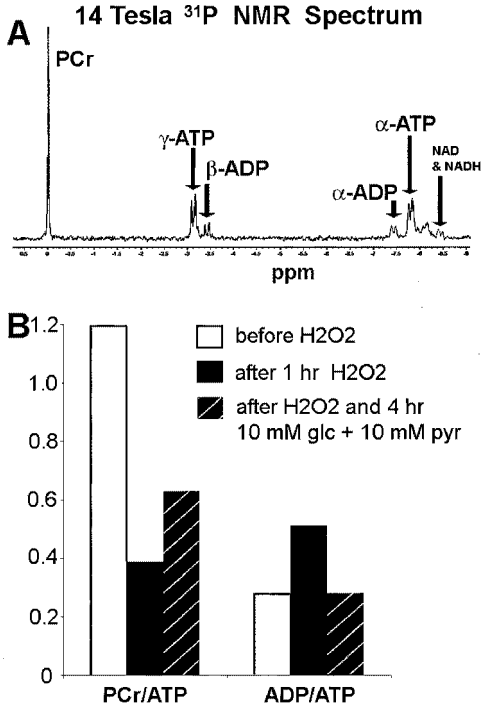

Fig. 1. (A) Region of a representative 14.1 Tesla ^{31}P NMR spectrum from slices before H_2O_2 exposure. Arrows show separately resolved ATP, ADP, and NAD doublet peaks, as described in the text. (B) Two metabolite ratios, PCr/ATP and ADP/ATP, are shown for three time points in a typical experiment, showing energy failure and recovery.

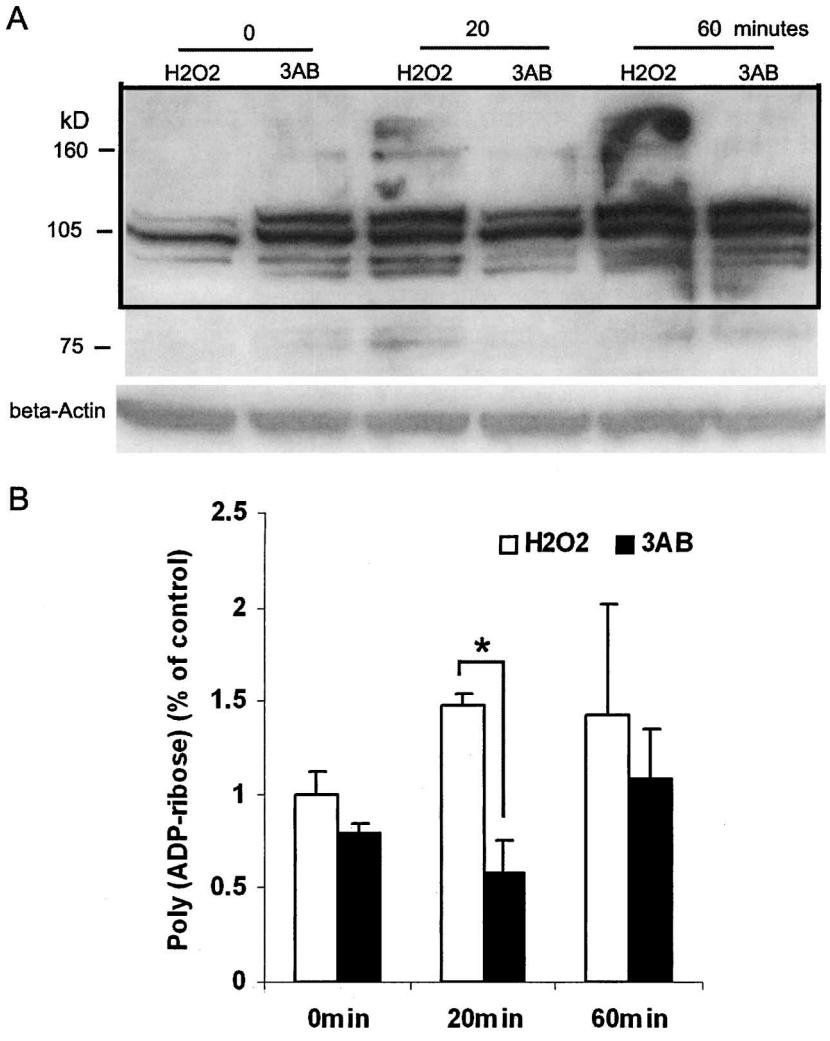

Fig. 2. (A) Representative Western blot showing PAR polymers in the molecular weight region included by the rectangle. Details are in the text. (B) Average OD ratios for three experiments, as described in the text. Bars show standard errors. *indicates significance at $p < 0.01$.

or 2-mM H_2O_2 for activation of PARP, while also maintaining our standard glucose concentration (10 mM) at all experimental times. We were successful in detecting PAR-polymer formation in those runs, but we did not start detecting energy failure and NAD depletion until the glucose concentration during H_2O_2 exposure was reduced to zero or 2 mM. Our results at this time are descriptive and qualitative, as can be seen first in Fig. 1, which shows representative data regarding energy failure, and Fig. 2, which shows representative Western blot data regarding PAR-polymer formation. The high NMR spectral resolsution of Fig. 1(A) makes it easy to discern that three energy metabolites of interest, ATP, ADP, and NAD, are doublets with a frequency separation of 18.5 Hz, the value known to arise in the pyrophosphate linkages that each contains. Each doublet is sufficiently resolved from its neighbors to permit quantification by direct integration. Figure 1(B) shows PCr/ATP and ADP/ATP ratios for three sets of slices in the same experiment, suggesting early energy failure at the 20 min point into H_2O_2 exposure and recovery afterwards. Because these ratios can be altered by the creating kinase reaction alone, metabolite quantifications rather than ratios are needed to assess energy failure. In the representative Western blot of Fig. 2(A), poly-(ADP-ribosylated)-proteins in the whole cell fraction, seen as diffuse immunoreactivity in the range of molecular weights outlined by the black rectangle, are markedly increased after 20- and 60-min exposures to 2 mM H_2O_2, but less increased, possibly unchanged, if treated as described with the PARP inhibitor 3AB (3 mM).

The same trend was found in three complete independent experiments, as shown in Fig. 2(B), where the ratio of (PAR polymers)/(β-actin) at $t = 20$ min was 1.48 ± 0.06, compared to 0.59 ± 0.17 ($p < 0.01$) in 3 mM 3AB-treated slices; and 1.43 ± 0.59 at $t = 60$ min compared to 1.08 ± 0.27 in 3AB-treated slices.

DISCUSSION

It should not be surprising that PARP activation in robust, well superfused, well-oxygenated brain slices did not appear to trigger the type of NAD^+ -depletion energy crisis seen in earlier cell culture studies, where availability of TCA metabolites might suffice in rescue (Ying *et al*., 2002). Indeed, PARP-1's actions are intertwined with many nonmetabolic mechanisms known to be important in hypoxic/ischemic injury, these including apoptosis and activation of rescue kinases and inflammatory mediators (Chiarugi and Moskowitz, 2003; Narasimhan *et al*., 2003; Yu *et al*., 2003). However, the brain slice system did reveal that it is amenable to accurate quantification of metabolite changes, and that with fine tuning of the model, energy failure and NAD^+ depletion (data not shown) can be made to occur. We note also that NMR spectroscopy, unlike enzymatic quantifications of NAD^+, measures only that NAD^+ which is freely mobile. Thus it seems possible that interesting information might come from comparisons of NMR and non-NMR NAD^+ quantifications. We find it noteworthy that total NAD^+ quantifications, without mention of redox ratios, have been emphasized in recent assessments of bioenergetic viability. It has long been known that there are many intricacies by which cells maintain a cytosolic [NAD^+]/[NADH] ratio appropriate for supplying lots of NAD^+ to glycolysis, while also maintaining a different mitochondrial ratio appropriate for supplying NADH to the electron transport chain (Newsholme, 1973). The use of ^{13}C-labeled nutrients in NMR bioenergetic studies might help provide insight to such things, because new high resolution NMR methods permit ^{13}C-labeled glycolytic and TCA intermediates to be identified and monitored via ^{1}H detection, which has considerably higher sensitivity (Burgess *et al*., 2001). In any event we find the preliminary data of this paper to be very encouraging about the establishment of brain slices paradigms for mechanistic studies, because PARP activation rapidly impairs glycolysis if exogenous TCA substrates are not available.

ACKNOWLEDGMENT

This work was supported by NIH grants R01 GM034767 (Dr Litt) and R01 NS041421 (Dr Swanson).

REFERENCES

Burgess, S. C., Carvalho, R. A., Merritt, M. E., Jones, J. G., Malloy, C. R., and Sherry, A. D. (2001). *Anal. Biochem.* **289**, 187–195.
Chiarugi, A., and Moskowitz, M. A. (2003). *J. Neurochem.* **85**, 306–317.
D'Amours, D., Desnoyers, S., D'Silva, I., and Poirier, G. G. (1999). *Biochem. J.* **342**, 249–268.
Davis, R. E., Mysore, V., Browning, J. C., Hsieh, J. C., Lu, Q. A., and Katsikis, P. D. (1998). *J. Histochem. Cytochem.* **46**, 1279–1289.
Eliasson, M. J. L., Sampei, K., Mandir, A. S., Hurn, P. D., Traystman, R. J., Bao, J., Pieper, A., Wang, Z.-Q., Dawson, T. M., Snyder, S. H., and Dawson, V. L. (1997). *Nat. Med.* **3**, 1089.
Endres, M., Wang, Z. Q., Namura, S., Waeber, C., and Moskowitz, M. A. (1997). *J. Cereb. Blood Flow Metab.* **17**, 1143–1151.
Hassa, P. O., and Hottiger, M. O. (2002). *Cell. Mol. Life Sci.* **59**, 1534–1553.
Herceg, Z., and Wang, Z. Q. (2001). *Mutat. Res.* **477**, 97–110.
Hirai, K., Sugawara, T., Chan, P. H., Basus, V. J., James, T. L., and Litt L. (2002). *J. Neurochem.* **83**, 309–319.
Litt, L., Hirai, K., Basus, V. J., and James, T. L. (2003). *Brain Res. Brain Res. Protoc.* **10**, 191–198.
Narasimhan, P., Fujimura, M., Noshita, N., and Chan, P. H. (2003). *Brain Res. Mol. Brain Res.* **113**, 28–36.
Newsholme, E. A. (1973). *Regulation in Metabolism*, Wiley, New York.
Virag, L., and Szabo, C. (2002). *Pharmacol. Rev.* **54**, 375–429.
Ying, W., Chen, Y., Alano, C. C., and Swanson, R. A. (2002). *J. Cereb. Blood Flow Metab.* **22**, 774–779.
Yu, S. W., Wang, H., Dawson, T. M., and Dawson, V. L. (2003). *Neurobiol. Dis.* **14**, 303–317.
Zhang, J., Dawson, V. L., Dawson, T. M., and Snyder, S. H. (1994). *Science* **263**, 687–689.